TUNABLE METAMATERIALS MADE OF GRAPHENE-LIQUID CRYSTAL MULTILAYERS

Amir Madani[1, 2, 3], Shuomin Zhong[1], Habib Tajalli[2], Samad R. Entezar[2], Abdolrahman Namdar[2], and Yungui Ma[1, *

[1]Center for Optical and Electromagnetic Research, State Key Lab of Modern Optical Instrumentation, Zhejiang University, Hangzhou 310058, China

[2]Faculty of Physics, University of Tabriz, P. O. Box 5167618949, Tabriz, Iran

[3]Department of Laser and Optical Engineering, University of Bonab, P. O. Box 5551761167, Bonab, Iran

Abstract—The dispersion properties of an anisotropic metamaterial composed of periodic stacking of graphene-liquid crystal layers are investigated in the far-infrared region. It is represented that this structure is able to show both the elliptic and hyperbolic dispersions using the tunable properties of the graphene and liquid crystal. The switching between two dispersion phases via control of the temperature, voltage and external electric field is studied. It is shown that this switching can be used to control of the transmission and reflection at the interface of the metamaterial and air.

1. INTRODUCTION

Hyperbolic dispersion or indefinite metamaterials (MMs) are a kind of anisotropic MMs in which different components of the permittivity and permeability tensors have opposite signs [1]. This results in an unusual hyperbolic dispersion relation for the medium and consequently many interesting phenomena such as hyperlensing [2–5], control of the electromagnetic fields [6], all-angle zero reflection [7, 8], all-direction pulse compression [9] and all-angle zero reflection-zero transmission [10] can be happened. Recently, the realization and

some properties of hyperbolic MMs are investigated using the MMs with periodic metal-dielectric layered structures and periodic metallic lines [11, 12]. One of the most important disadvantages of such structures is the lack of tunability and switching properties. Besides, high dissipative loss of MMs due to the presence of the metal layers is another problem of these structures.

This problems can be overcome if materials with low loss and tunable optical parameters are used in the layered structures. More recently, Li et al. have investigated a switchable hyperbolic MM with magnetic control using a periodic gyromagnetic-dielectric layered structure [10]. They have shown that the dispersion relation of the structure can be switched between hyperbolic and elliptic phases via d.c. magnetic control and the dissipative loss of the MM is lower than the metallic structures in the microwave region.

Graphene, an allotrope of carbon atoms arranged in one atom thick honey-comb lattice [13], can be introduced as another alternative to lossy metallic layers. Beside the general features such as high mobility of carriers, flexibility, robustness and environmental stability [14, 15], graphene has some properties which can make it a suitable option in designing photonic devices and hyperbolic MMs. At the frequency ranges of THz and far-infrared, the dissipative loss of graphene is less than the usual metals and its optical response is described by the surface conductivity which is related to its chemical potential and can be controlled and tuned by voltage or chemical doping [16–18]. Graphene-based liquid crystal devices, optical modulators and switches can be mentioned as examples [19–22]. Also, the optical properties and some applications of the multilayer graphene structures have been investigated by different research groups. For example, Wang et al. investigated the coupling between surface plasmon polaritons in a multilayer graphene sheet arrays [18]. Graphene hyperlens for THz radiation have been proposed by Andryieuski using graphene-dielectric multilayered stack [23]. Iorsh et al. suggested a kind of hyperbolic MMs where individual graphene sheets are separated by host dielectric slabs and demonstrated a possibility of tuning the dispersion properties of the MM with external electric and magnetic fields [24]. The tunability of the reflection and transmission properties of a film made of graphene-dielectric multilayer structure at THz frequencies have been investigated by Othman et al. [25].

On the other hand, liquid crystals (LCs) as a kind of uniaxial nonmagnetic dielectric materials with tunable optical properties [26], are good choices to be used in the mentioned layered MMs. The permittivity components of the LC molecules are temperature

dependent and the anisotropy of the material can be easily controlled by the electric fields [26–28]. Consequently, the optical response of the whole MM structure is modified.

So, in the present paper, we study the dispersion properties of a kind of hyperbolic MMs composed of periodic graphene-LC layered structure. The major advantage of this MM structure comparing with the previously mentioned ones is the possibility of the thermal controlling of the dispersion properties of the MM. The effects of the temperature, external electric field and voltage in the dispersion behavior of the MM are investigated. It is found that the dispersion of the structure can be switched between hyperbolic and elliptic phases via control of the mentioned parameters. Also, the possibility of using this structure as a switchable all-angle total transmitter is shown by the simulation.

2. THEORETICAL MODEL

The model of our MM is represented in Fig. 1. It is a graphene multilayer structure in which the spaces between graphene sheets are assumed to be filled with LC material. This may be done using vacuum filling method which is a well-known technique in the experimental study of liquid crystals [29]. So, the structure can be considered as a periodic stacking of graphene monolayers and LC (dielectric) layers. The thicknesses of the graphene, $d_1 = 1\,\text{nm}$, and the LC layer, $d_2 = 20\,\text{nm}$, are assumed to be much smaller than the operating wavelength, $\lambda = 10.6\,\mu\text{m}$, and satisfying the homogeneous effective medium approximation.
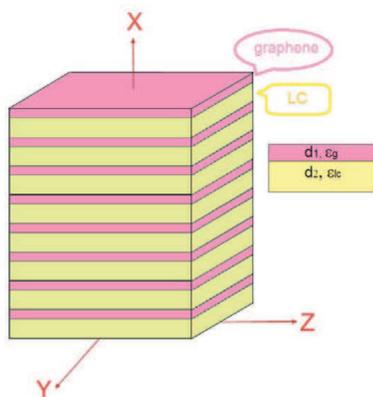
Figure 1. The model of MM structure which is a periodic stacking of graphene and LC layers.

The effective permittivity of the graphene is shown by ε_g and the permittivity of the LC is given by diagonal tensor, $\bar{\bar{\varepsilon}}_{LC} =$ diag$[\varepsilon_{lcx}, \varepsilon_{lcy}, \varepsilon_{lcz}]$. This periodic structure can be viewed as an effective anisotropic MM with the permittivity tensor as $\bar{\bar{\varepsilon}}_{eff} =$ diag$[\varepsilon_x, \varepsilon_y, \varepsilon_z]$ [30], where

$$\varepsilon_x = \frac{\varepsilon_g \varepsilon_{lcx}(d_1 + d_2)}{\varepsilon_g d_2 + \varepsilon_{lcx} d_1} \quad \varepsilon_i = \frac{\varepsilon_g d_1 + \varepsilon_{lci} d_2}{(d_1 + d_2)} \tag{1}$$

and $i = y, z$. The permeability of the effective anisotropic MM is assumed to be $\mu = 1$. In this work only transverse magnetic (TM) mode is considered and we assume a plane wave with the magnetic field of the form $\mathbf{H} = H_y \exp[i(k_x x + k_z z) - \omega t]\hat{y}$. Using the Maxwell equations

$$\nabla \times \mathbf{E} = -\mu \frac{\partial \mathbf{H}}{\partial t}, \quad \nabla \times \mathbf{H} = \bar{\bar{\varepsilon}}_{eff} \frac{\partial \mathbf{E}}{\partial t}, \tag{2}$$

the following wave equation is obtained inside the effective MM:

$$\nabla \times \left(\varepsilon^{-1} \nabla \times \mathbf{H}\right) = -\mu \frac{\partial^2 \mathbf{H}}{\partial t^2}. \tag{3}$$

By using simple algebra, the dispersion relation of the effective MM can be derived as:

$$\frac{k_x^2}{\varepsilon_z} + \frac{k_z^2}{\varepsilon_x} = \frac{\omega^2}{c^2}. \tag{4}$$

The sign of ε_x and ε_z are dependent on the optical parameters of the graphene and LC layers and from Eq. (4), one can find that the dispersion of the structure is hyperbolic when $\varepsilon_x \varepsilon_z < 0$ and is elliptic when $\varepsilon_x \varepsilon_z > 0$.

The graphene is considered as ultrathin metallic layers with the relative equivalent permittivity of $\varepsilon_g = 1 + i\sigma_g \eta_0/(k_0 d_1)$ where $k_0 = 2\pi/\lambda$ is the vacuum wavevector, η_0 is the impedance of air and σ_g is the surface conductivity of the graphene [18]. σ_g is obtained from the Kubo formula [31] including the intraband and interband transition contributions as $\sigma_g(\omega) = \sigma_g^{intra}(\omega) + \sigma_g^{inter}(\omega)$, where

$$\sigma_g^{intra}(\omega) = \frac{e^2}{4\hbar} \frac{i}{2\pi} \left\{ \frac{16 k_B T}{\hbar\omega} \ln\left(2\cosh\left(\frac{\mu_c}{2k_B T}\right)\right) \right\},$$

$$\sigma_g^{inter}(\omega) = \frac{e^2}{4\hbar} \left\{ \frac{1}{2} + \frac{1}{\pi} \arctan\frac{\hbar\omega - 2\mu_c}{2k_B T} - \frac{i}{2\pi} \ln\frac{(\hbar\omega + 2\mu_c)^2}{(\hbar\omega - 2\mu_c)^2 + (2k_B T)^2} \right\}. \tag{5}$$

Here, e is the charge of an electron, k_B the Boltzmann constant, T the temperature in K, and μ_c the chemical potential which we assume to take the values between 0.1–0.5 eV [33]. These expressions show that

the interband contribution plays the leading role around the absorption threshold, $\omega \approx 2\mu$, while the intraband contribution is important at relatively low frequencies, $\omega < 2\mu$. Recently, it has been demonstrated that the spatial dispersion of graphene may have influence on the propagation of electromagnetic waves, but this effect is negligible when the graphene sheets are surrounded by low permittivity dielectrics [32]. So, we neglect the spatial dispersion effect in our study.

We consider the mostly used commercial liquid crystal mixture E7, with a wide nematic temperature range (263 K to 331 K), as a constituent of the dielectric layers. At $\lambda = 10.6\,\mu\text{m}$, the ordinary (n_o) and extraordinary (n_e) refractive indices of E7 are determined around 1.5 and 1.7, respectively. As mentioned earlier the n_o and n_e of the LC are temperature dependent and can be shown as [27, 28]:

$$
\begin{aligned}
n_e(T) &\simeq a - bT + \frac{2}{3}(\triangle n)_0 \times S \\
n_o(T) &\simeq a - bT - \frac{1}{3}(\triangle n)_0 \times S
\end{aligned}
\tag{6}
$$

where $S = (1 - \frac{T}{T_c})^\beta$ is the order parameter, T_c is the phase transition point in K, β a constant coefficient which depends on the LC material, $(\triangle n)_0$ the birefringence at $T = 0\,\text{K}$, and a and b are two parameters obtained by fitting the experimental and theoretical data. For E7 nematic LC, $T_c = 331\,\text{K}$ and the fitting parameters at the operating wavelength, $\lambda = 10.6\,\mu\text{m}$, are obtained as: $a = 1.7201$, $b = 2.25 \times 10^{-4}\,(1/\text{K})$, $(\triangle n)_0 = 0.3499$ and $\beta = 0.2579$ [27]. The imaginary parts of the extraordinary and ordinary refractive indexes at the given wavelength are assumed as $\kappa_e = 9.28 \times 10^{-3}$ and $\kappa_o = 6.75 \times 10^{-3}$, respectively [34].

3. RESULTS AND DISCUSSION

The optical properties of the graphene depend on its surface conductivity. The conductivity can be varied by adjusting the chemical potential, which is governed by the carrier density. The carrier density can be changed by either chemical doping or by the application of a bias voltage. So, one can tune ε_g by the control of the chemical potential via voltage tuning and this leads to the modification of the dispersion properties of our MM structure.

To see this effect, we suppose that the voltage is applied to the graphene layers along the $\hat{x}$ direction and μ_c can be tuned between 0.1 eV to 0.5 eV. In the experimental realization, this voltage may be provided by electrodes which are THz transparent dc conductors such as thin doped InSb films [24, 35]. However, these materials show some

limitations in the temperature and frequency ranges and the solution of this problem is the subject of a new study. The LC molecules are also oriented in this direction under the influence of the electric field and the components of the permittivity tensor of the LC are defined by $\varepsilon_{lcx} = \varepsilon_e$, $\varepsilon_{lcy} = \varepsilon_o$ and $\varepsilon_{lcz} = \varepsilon_o$ where ε_o and ε_e are the ordinary and extraordinary permittivity constants, respectively. In Fig. 2(a), the equifrequency curves of the dispersion relation (Eq. (4)) are plotted as a function of the μ_c at room temperature ($T = 300\,\mathrm{K}$) and the given wavelength, $\lambda = 10.6\,\mu\mathrm{m}$. It is evident from the figure that the dispersion of the MM can be controlled and switched between ellipticity and hyperbolicity via control of the voltage. The curves are elliptic for a small range of low value chemical potentials, while by increasing the voltage they will change into hyperbolic at $\mu_c > 0.122\,\mathrm{eV}$ (magenta curve). Further increase of μ_c, modifies the shape of the curves but doesn't change the dispersion type of the MM. Here, the lower μ_c are shown by the bluish colors while the reddish ones show the higher μ_c. This switchability is the great advantage of the using graphene instead of the conventional metals in the layered MM structures and can have many potential application in the control of the electromagnetic waves and designing the graphene-based switchable devices such as hyperlenses.
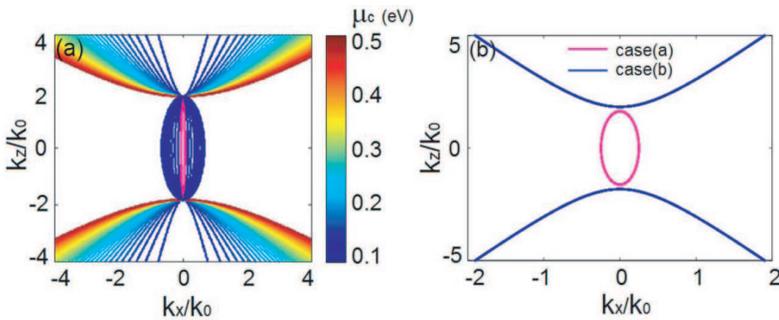
Figure 2. (a) The equifrequency curves of the dispersion relation as a function of μ_c and (b) the equifrequency curve of the dispersion relation for the cases a (magenta curve) and b (blue curve) of the LC orientation at a given wavelength, $\lambda = 10.6\,\mu\mathrm{m}$ and room temperature ($T = 300\,\mathrm{K}$).

Strong sensitivity and response to the external electric fields is one of the major characteristics of nematic LCs which has so many applications in the photonics and optoelectronics. By applying an electric field, the LC molecules tend to align along the direction of the

field and in conventional electro-optical devices, a field, on the order of a few (volts/μm) [36], is sufficient to rotate the director axis of the LC around 90°. This small value of the external field has not significant effect in the chemical potential of the graphene multilayers [17]. In our case, the reorientation of LC molecules influences the anisotropy of the medium and leads to the modification of the optical and dispersion properties of the MM structure. So, we study this effect by investigating the dispersion of the MM for two cases of the LC directions at room temperature. We use the same chemical potential $\mu_c = 0.15\,\text{eV}$ for both cases.

In the case (a), we assume that the LC molecules are aligned in the plane of the interfaces using a d.c. electric field and their director is along the $\hat{z}$ direction. Here, we consider chemically doped graphene sheets with $\mu_c = 0.15\,\text{eV}$ and the other parameters as the same as mentioned earlier. In the case (b), we consider pure graphene sheets with a stronger gate voltage to prepare chemical potential of $0.15\,\text{eV}$. Consequently, the LC molecules are aligned perpendicular to the layers under the influence of this field and their director is along the direction of $\hat{x}$. So, the permittivity of the LC is shown by $\bar{\varepsilon}_{LC} = \text{diag}[\varepsilon_o, \varepsilon_o, \varepsilon_e]$ for the case (a) and $\bar{\varepsilon}_{LC} = \text{diag}[\varepsilon_e, \varepsilon_o, \varepsilon_o]$ for the case (b).

In Fig. 2(b), the equifrequency curves of the dispersion relation (Eq. (4)) are plotted for the cases a (magenta curve) and b (blue curve) at the given wavelength and room temperature. The possibility of the switching between elliptic and hyperbolic dispersions by the reorientation of the LC molecules is obvious from the figure. The MM has the elliptic dispersion relation for the case (a) while it can be changed simply to the hyperbolic via the external electric field application.

LCs, as a kind of anisotropic nonmagnetic dielectric materials, have temperature dependent dielectric constants. This tunability is an advantage of the LCs comparing with the other dielectric materials and has many applications in the optical switching and sensing devices. Meanwhile, our numerical analysis showed that the temperature dependent variation of the graphene conductivity (Eq. (5)) is negligible around the room temperature. Here, we study the effect of the temperature on the dispersion properties of our MM structure. It is assumed that the nematic LC molecules are aligned parallel to the $\hat{z}$ direction and the chemical potential of the doped graphene is taken as $\mu_c = 0.15\,\text{eV}$. In Fig. 3(a), the temperature dependence of the values of ε_x, ε_z and $\varepsilon_x\varepsilon_z$ are represented in the range of $300\,\text{K}$ to $320\,\text{K}$.

It is evident from the figure that ε_x is always positive in the given temperature region, but the sign of ε_z and consequently the sign of $\varepsilon_x\varepsilon_z$, are changed from + to − near the $312\,\text{K}$ by increasing the

temperature. This different behavior is due to the different forms of ε_x and ε_z (Eq. (1)) and also opposing temperature gradients of ε_o and ε_e of the LC material (Eq. (6)). As mentioned before, this will result in the considerable change in the dispersion behavior of the anisotropic MM.
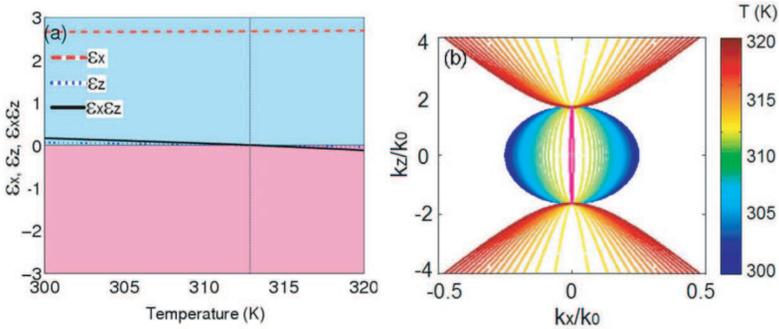
Figure 3. (a) The temperature dependence of ε_x, ε_z and $\varepsilon_x\varepsilon_z$, (b) the equifrequency curves of the dispersion relation as a function of temperatures at a given wavelength, $\lambda = 10.6\,\mu\text{m}$ and chemical potential $\mu_c = 0.15\,\text{eV}$.

To show this effect more clearly, in Fig. 3(b), the equifrequency curves of the dispersion relation (Eq. (4)) are plotted as a function of the temperature at the used wavelength. In the figure, the higher and the lower temperatures are shown by the reddish and bluish colors, respectively. It is obvious from the figure that the elliptic dispersion of the MM is gradually switched to the hyperbolic one via the increase of the temperature. The switching temperature in this case is around 312 K and the corresponding dispersion curve is shown by the magenta color in the figure. It is evident that in the neighborhood of the switching point the dispersion curves are restricted to the very small values of k_x, i.e., only the waves with the propagation direction around the $\hat{z}$ can propagate inside the MM. But, with going away from the switching temperature, the waves with the larger k_x can also have propagation in the MM.

As mentioned before, one potential application of the dispersion switching in the MM is the control of the reflection and transmission at the terminating surface of the MM. It is shown that for an anisotropic hyperbolic dispersion MM, reflection is dependent on the surface termination angle of the MM [7, 10]. In other words, it depends on the angle between the interface and the asymptote of the hyperbolic dispersion curve. If the surface of our MM is cut perpendicularly to

one of the asymptote, the zero reflection condition is fulfilled for all incident angles and we have an all-angle total transmitter which can be tuned by the controlling parameters.

To illustrate this critical condition, we consider a new coordinate system (x', y', z') by rotating the principle system by the angle of θ around y axis. In this new system, the permittivity tensor of the effective anisotropic MM is obtained as:

$$\bar{\varepsilon}' = \begin{pmatrix} \varepsilon_{x'x'} & \varepsilon_{x'z'} \\ \varepsilon_{z'x'} & \varepsilon_{z'z'} \end{pmatrix} = \begin{pmatrix} \varepsilon_x C^2 + \varepsilon_z S^2 & CS(\varepsilon_x - \varepsilon_z) \\ CS(\varepsilon_x - \varepsilon_z) & \varepsilon_x S^2 + \varepsilon_z C^2 \end{pmatrix} \quad (7)$$

where, $C \equiv \cos(\theta)$ and $S \equiv \sin(\theta)$. Using the Maxwell equations, the dispersion relation in new coordinate system is obtained as:

$$\frac{\varepsilon_{x'x'} k_{x'}^2 + \varepsilon_{z'z'} k_{z'}^2 + 2\,\varepsilon_{x'z'} k_{x'} k_{z'}}{\varepsilon_{x'x'} \varepsilon_{z'z'} - \varepsilon_{x'z'}^2} = \frac{\omega^2}{c^2} \quad (8)$$

where, $k_{x'}$ and $k_{z'}$ are the components of the propagation vector along x' and z', respectively. The critical condition is defined as $\theta = \theta_c = \arctan(\sqrt{|\frac{\varepsilon_z}{\varepsilon_x}|})$, in which the equifrequency dispersion curve in the new coordinate system have a perpendicular asymptote to the x' axis.

For the case of perpendicular orientation of the LC molecules to the layers at room temperature and other parameters used in this work, $\theta_c = 22.2°$ is calculated and the equifrequency dispersion curve in new coordinate system is plotted in Fig. 4(a). It is evident from the figure that the x' axis is perpendicular to the one of the asymptote of the hyperbolic dispersion. Therefore, if the MM surface is terminated normally to z' axis, i.e., in the $(x'\text{-}y')$ plane, the condition of all-angle zero reflection is fulfilled for the waves incident from the MM to the interface.

To show more about this effect, the FDTD simulation results of our model are represented in Fig. 4(b) to Fig. 4(d) where we have used a TM polarized Gaussian beam with the wavelength of $\lambda = 10.6\,\mu m$. Fig. 4(b) to Fig. 4(d) are related to the incidence situations shown in Fig. 4(a) and corresponding to the incidence angles, $\theta_{inc} = 22.2° = \theta_c$, $\theta_{inc} = 12° < \theta_c$ and $\theta_{inc} = 35° > \theta_c$, respectively. θ_{inc} is defined as the angle between incident wave and the normal to the interface of MM (left part) and air (right part). The simulation results show the zero reflection for all of the three incident waves and confirm the all-angle or θ_{inc}-independent total transmission of our MM structure in the critical condition. As mentioned in the previous sections, the dispersion of the MM can be switched to the elliptic form by changing the director orientation of the LCs or tuning the voltage, so the total transmission condition is switched off. Unlike the total transmission condition,
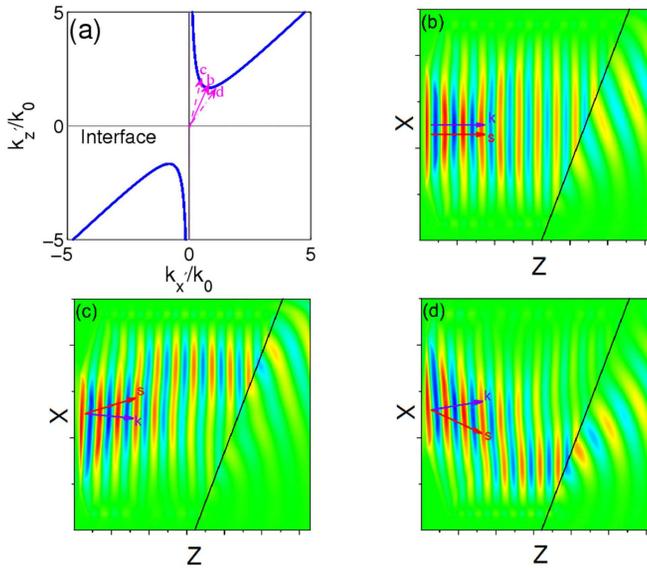
Figure 4. (a) The equifrequency dispersion curve in the new coordinate system for the case of critical condition, $\theta = \theta_c$. It is assumed that the LC molecules are oriented perpendicular to the layers at room temperature. (b), (c) and (d) FDTD simulations of the magnetic field distribution for a TM polarized Gaussian beam which is incident from MM to the interface of MM (left) and air (right) corresponding to the incidence angles, $\theta_{inc} = 22.2° = \theta_c$, $\theta_{inc} = 12° < \theta_c$ and $\theta_{inc} = 35° > \theta_c$, respectively.

the direction of the the phase and group velocities (wave vector and pointing vector) of the electromagnetic waves in the anisotropic MM is completely dependent on the θ_{inc}. These directions for the cases of b, c and d are represented by the $\vec{k}$ and $\vec{s}$ vectors in the figures, respectively. For the case b, where the incidence angle of the beam is equal to the critical angle ($\theta_{inc} = \theta_c$), the $\vec{k}$ and $\vec{s}$ are completely parallel, while, unparalleled directions of them are evident for the cases of c and d.

4. CONCLUSION

In summary, the dispersion properties of the MM composed of graphene-LC periodic layers are investigated for the TM polarized waves. The permeability of the LC and the surface conductivity of the graphene sheets are tunable parameters. So, the optical

parameters of the effective structure can be controlled and the MM is able to show both the elliptic and hyperbolic dispersion depending on the optical constants of the constituent materials. The effects of the temperature, voltage and external electric field on the optical constants and consequently, on the dispersion of the MM are studied. Our calculation shows that the dispersion of the MM can be easily switched between elliptic and hyperbolic via control of the mentioned parameters. Hyperbolic dispersion materials have some applications in the design of hyperbolic devices such as hyperlenses. Besides, the switching between elliptic and hyperbolic dispersion results in the tunability of these devices. For example, it may have many applications in the control of the electromagnetic fields at the surface of the MM. Our simulation results show that the graphene-LC multilayer structure has zero reflection for all incident angles if the surface of the MM is cut in a critical condition. In this case, it can work as a tunable all-angle total transmitter.

ACKNOWLEDGMENT

REFERENCES

1. Smith, D. R. and D. Schurig, "Electromagnetic wave propagation in media with indefinite permittivity and permeability tensors," *Phys. Rev. Lett.* , Vol. 90, 077405-4, 2003.

2. Jacob, J., L. Alekseyev, and E. Narimanov, "Optical hyperlens: Far-field imaging beyond the diffraction limit," *Opt. Express*, Vol. 14, 8247–8256, 2006.

3. Liu, Z. W., H. Lee, Y. Xiong, C. Sun, and X. Zhang, "Far-field optical hyperlens magnifying sub-diffraction-limited objects," *Science*, Vol. 315, 1668, 2007.

4. Li, X., Y. Ye, and Y. Jin, "Impedance-mismatched hyperlens with increasing layer thicknesses," *Progress In Electromagnetics Research*, Vol. 118, 273–286, 2011.

5. Wheeland, S., A. V. Amirkhizi, and S. Nemat-Nasser, "Soft-focusing in anisotropic indefinite media through hyperbolic dispersion," *Progress In Electromagnetics Research*, Vol. 132, 389–402, 2012.

6. Sun, J., B. Sun, H. Li, L. W. Chan, J. Zhou, and Y. Wang, "Controlling the electromagnetic field by indefinite media with extremely strong anisotropy," *Progress In Electromagnetics Research*, Vol. 130, 513–524, 2012.

7. Li, X., Z. Liang, X. Liu, X. Jiang, and J. Zi, "All-angle zero reflection at metamaterial surfaces," *Appl. Phys. Lett.*, Vol. 93, 171111-3, 2008.

8. Yang, J., X. Hu, X. Li, Z. Liu, X. Jiang, and J. Zi, "Cancellation of reflection and transmission at metamaterial surfaces," *Opt. Lett.*, Vol. 35, 16–18, 2010.

9. Liu, Z., Z. Liang, X. Jiang, X. Hu, X. Li, and J. Zi, "Hyper-interface, the bridge between radiative wave and evanescent wave," *Appl. Phys. Lett.*, Vol. 96, 113507-3, 2010.

10. Li, W., Z. Liu, X. Zhang, and X. Jiang, "Switchable hyperbolic metamaterials with magnetic control," *Appl. Phys. Lett.*, Vol. 100, 161108-4, 2012.

11. Salandrino, A. and N. Engheta, "Far-field subdiffraction optical microscopy using metamaterial crystals: Theory and simulations," *Phys. Rev. B*, Vol. 74, 075103-5, 2006.

12. Yao, J., Z. Liu, Y. Liu, Y. Wang, C. Sun, G. Bartal, A. M. Stacy, and X. Zhang, "Optical negative refraction in bulk metamaterials of nanowires," *Science*, Vol. 321, 930, 2008.

13. Novoselov, K., A. Geim, S. Morozov, D. Jiang, Y. Zhang, S. Dubonos, I. Grigorieva, and A. Firsov, "Electric field effect in atomically thin carbon films," *Science*, Vol. 306, 666–669, 2004.

14. Geim, A., "Graphene: Status and prospects," *Science*, Vol. 324, 1530–1534, 2009.

15. Bonaccorso, F., Z. Sun, T. Hasan, and A. C. Ferrari, "Graphene photonics and optoelectronics," *Nat. Photon.*, Vol. 4, 611–622, 2010.

16. Hanson, G. W., "Quasi-transverse electromagnetic modes supported by a graphene parallel-plate waveguide," *J. Appl. Phys.*, Vol. 104, 084314-5, 2008.

17. Hanson, G. W., "Dyadic Greens functions for an anisotropic, non-local model of biased graphene," *IEEE Trans. Antennas Propagat.*, Vol. 56, 747–757, 2008.

18. Wang, B., X. Zhang, F. Garcya-Vidal, X. Yuan, and J. Teng, "Strong coupling of surface plasmon polaritons in monolayer graphene sheet arrays," *Phys. Rev. Lett.*, Vol. 109, 073901-5, 2012.

19. Blake, P., P. Brimicombe, R. Nair, T. Booth, D. Jiang, F. Schedin, L. Ponomarenko, S. Morozov, H. Gleeson, E. Hill, A. Geim, and

K. Novoselov, "Liquid crystal addressing by graphene electrodes made from graphene oxide," *Nano Lett.*, Vol. 8, 100206-3, 2008.

20. Liu, M., X. Yin, E. Ulin-Avila, B. Geng, T. Zentgraf, L. Ju, F. Wang, and X. Zhang, "A graphene-based broadband optical modulator," *Nature*, Vol. 474, 64–67, 2011.

21. Ren, L., Q. Zhang, J. Yao, Z. Sun, R. Kaneko, Z. Yan, S. Nanot, Z. Jin, I. Kawayama, M. Tonouchi, J. Tour, and J. Kono, "Terahertz and infrared spectroscopy of gated large-area graphene," *Nano Lett.*, Vol. 12, 3711–3715, 2012.

22. Lee, S. H., M. Choi, T. T. Kim, S. Lee, M. Liu, X. Yin, H. Choi, S. Lee, C. G. Choi, S. Y. Choi, X. Zhang, and B. Min, "Switching terahertz waves with gate-controlled active graphene metamaterials," *Nat. Mater.*, Vol. 11, 936–941, 2012.

23. Andryieuski, A., A. V. Lavrinenko, and D. N. Chigrin, "Graphene hyperlens for terahertz radiation," *Phys. Rev. B*, Vol. 86, 121108(R)–5, 2012.

24. Iorsh, I. V., I. S. Mukhin, I. V. Shadrivov, P. V. Belov, and Y. S. Kivshar, "Hyperbolic metamaterials based on multilayer graphene structures," *Phys. Rev. B*, Vol. 87, 075416-6, 2013.

25. Othman, M. A. K., C. Guclu, and F. Capolino, "Graphene-based tunable hyperbolic metamaterials and enhanced near-field absorption," *Opt. Express*, Vol. 21, 7614–7632, 2013.

26. Khoo, I. C. and S. T. Wu, *Optics and Nonlinear Optics of Liquid Crystals*, World Scientific, Singapore, 1993.

27. Li, J., S., Wu, S. Brugioni, R. Meucci, and S. Faetti, "Infrared refractive indices of liquid crystals," *J. Appl. Phys.*, Vol. 97, 073501-5, 2005.

28. Yang, C., C. Lin, R. Pan, C. T. Que, K. Yamamoto, M. Tani, and C. Pan, "The complex refractive indices of the liquid crystal mixture E7 in the terahertz frequency range," *J. Opt. Soc. Am. B*, Vol. 27, 1866–1872, 2010.

29. Wu, W., C. Chang, H. Cheng, C. Hsu, and K. Tsen, "Continuous cell air-extracting technique used for fast cell filling of flexible liquid-crystal displays," *J. Vac. Sci. Technol. B*, Vol. 28, 673–677, 2010.

30. Wang, S. and L. Gao, "Omnidirectional reflection from the one-dimensional photonic crystal containing anisotropic left-handed material," *Eur. Phys. J. B*, Vol. 48, 29–36, 2005.

31. Falkovsky, L. and S. Pershoguba, "Optical far-infrared properties of a graphene monolayer and multilayer," *Phys. Rev. B*, Vol. 76, 153410-4, 2007.

32. Gomez-Diaz, J., J. Mosig, and J. Perruisseau-Carrier, "Effect of spatial dispersion on surface waves propagating along graphene sheets," *IEEE Trans. Antennas Propag.*, Vol. 61, 3589–3596, 2013.

33. Chen, P. Y. and A. Alu, "Atomically thin surface cloak using graphene monolayers," *ACS Nano*, Vol. 5, 5855–5863, 2011.

34. Brugioni, S. and R.Meucci, "Liquid crystals in the mid-infrared region and their applications," *Infrared Phys. Technol.*, Vol. 46, 17–21, 2004.

35. Wang, X., A. Belyanin, S. Crooker, D. Mittleman, and J. Kono, "Interference-induced terahertz transparency in a semiconductor magneto-plasma," *Nat. Phys.*, Vol. 6, 126–130, 2009.

36. Khoo, I. C., "Nonlinear optics of liquid crystalline materials," *Phys. Rep.*, Vol. 471, 221–276, 2009.